Electronic Supplementary Information (ESI)

for

A Nanocarbon-Enabled Hybridization Strategy to Construct Pharmacologically Cooperative Therapeutics for Augmented Anticancer Efficacy

Huan Wang,[1] *Xinchen Liu,*[2] *Xiangyu Yan,*[3] *Yong Du,*[3] *Fang Pu,*[1] *Jinsong Ren,**[,1] *Xiaogang Qu**[,1]

1. A State Key Laboratory of Rare Earth Resources Utilization and Laboratory of Chemical Biology, Changchun Institute of Applied Chemistry, Chinese Academy of Sciences, Changchun, Jilin 130022, P. R. China E-mail: *jren@ciac.ac.cn; *xqu@ciac.ac.cn
2. Jilin Provincial Key Laboratory of Tooth Development and Bone Remodeling, Hospital of Stomatology, Jilin University, Changchun, Jilin 130021, P. R. China
3. State Key Laboratory of Powder Metallurgy, Central South University, Changsha, Hunan 410083, P. R. China

I. Methods

Metadynamics simulations

To determine the final structure of SCACDs, we carried out analysis by molecular dynamics and DFT calculations, comparing and combining them with the characterization results. The simulation of the chemical reaction by the hydrothermal process was simulated by the CP2K (v2023.1) program incorporated with PLUMED for molecular dynamics simulation with metadynamics method.[1, 2] We employed the plane-wave cut-off as 600 Ry and added DZVP-MOLOPT-SR-GTH as the mixed basis set. The criterion for SCF was set as 10^{-5} Ry. The functional was selected as PBE combined with D3 correction for the weak interactions.[3, 4] A semi-empirical method was applied to deal with this large system in the following simulation describing carbon core formation, which was the Geometry, Frequency and Noncovalent interaction Extended Tight Binding (GFN-xTB) by Grimme et al..[5] We employed the metadynamics method in both the reaction of the sulfasalazine with the citric acid (stage 1) and the following carbon core simulation (stage 2). The time step of these simulations was set as 1 fs under 473 K in terms of our hydrothermal reaction condition.

The metadynamics proposed by Laio and Parrinello is prevailed in latest years to enhance sampling during molecular dynamics simulation presented in Equation (1) and (2).[6]

$$H(x,t) = H(x) + V(\xi,t) \tag{1}$$

$$V(\xi,t) = w\sum_{i=1}^{t/t_G} \exp\left(-\frac{|\,\xi^{(t)} - \xi^{(i\mathfrak{g}_G)}(x)\,|^2}{2\sigma^2} \right) \tag{2}$$

$H(x)$ is the Hamiltonian for the original system and $V(\xi,t)$ is the time-dependent biased potential. The w and σ are the height and width of Gaussian hills of the added biased potential, t_G is the time increment of adding a Gaussian hill. The biased potential in terms of $\xi^{(t)}$ named as collective variables (CV) is mandatory in this simulation defining the degrees of freedom in the system. The CV1 of stage 1 is the coordination number as shown in Equation (3),

$$s = \frac{1-(r/r_0)^n}{1-(r/r_0)^m} \tag{3}$$

Here r is the distance between each atom, r_0 (C-C 2.68 Bohr) is the standard distance between each atom. The m and n are defined as 14 and 8, respectively. Here, the very large height of the Gaussian hills with 0.3 Hartree is applied in this system at every 40 molecular dynamics steps to efficiently observe the carbonization process at 473 K, while the Gaussian width is 0.2. The CV2 of stage 2 is SPRINT method to simulate the carbon core formation

with fractured groups, the CV2 is defined as:[7]

$$s_i = \sqrt{N}\lambda v_i \quad (4)$$

In Equation (4), N is the total number of atoms, λ and v_i represent the eigenvalue and eigenvector in contact matrix between different atoms, λ is selected as the largest eigenvalue while v_i is the largest eigenvector in the calculation. The NxN matrix consists of all possible distances between atoms. The height and width of Gaussian hills in stage 2 are 0.003 Hartree and 0.8 respectively at every 100 molecular dynamics steps. This total simulation time is 220 ps.

NMR and UV-Vis calculations

The NMR and adsorption spectrum calculations were performed by Gaussian 16 Rev. C 01.[8] The NMR calculation was based on the gauge-independent atomic orbital (GIAO) methodology.[9] All the molecules underwent geometric optimization based on B3LYP functional with 6-31g(d,p) basis set at gas phase. Then the NMR calculations were based on B97-2 and revTPSS functional with pcSseg-1 basis set using the SMD model for chloroform.[10, 11] The chemical shift,

$$\delta_i = \sigma_{ref} - \sigma_i + \delta_{ref}$$

Where the σ_{ref} and σ_i are the isotropic shifts of the reference molecule and interested molecules respectively. And the δ_{ref} is the chemical shift of the reference molecule. Here we used the Tetramethylsilane (TMS) as the standard reference molecule ($\delta_{ref} = 0$). The time-dependent DFT (TDDFT) calculations were based on the CAM-B3LYP functional with 6-31g(d,p) basis set by SMD model for water. We used the VMD to present the images in our study and the Multiwfn as assistance for dealing the calculation data.[12, 13]

Materials

The sulfasalazine (≥98%) and citric acid monohydrate (AR, 99.5%) were purchased from Aladdin Reagent. The DSPE-mPEG (M_W = 5000) and DSPE-PEG-Cy5 (M_W = 5000) were ordered from ToYong Biotechnology. The ammonia solution (25~28%) was purchased from XiLONG Scientific. Ultrapure (UP) water was prepared the by Milli-Q-Plus system (18.2 MΩ cm^{-1}) and used throughout all the experiments. The Goat Serum, TUNEL Apoptosis Assay Kit, and Phospho-AMPKα1 (Thr183)/AMPKα2 (Thr172) polyclonal antibody were purchased from Beyotime Biotechnology. Cystine Uptake Assay Kit was purchased from DOJINDO Laboratories. The ROS indicator DCFH-DA was purchased from Sigma Aldrich. The GPX4 polyclonal antibody, LC3 recombinant

antibody, AMPKα1 monoclonal antibody, Beclin 1 monoclonal antibody, GAPDH monoclonal antibody, β-actin monoclonal antibody, HRP-conjugated secondary antibodies were purchased from Proteintech Group, Inc.. DyLight 488-conjugated secondary antibodies and DyLight 550-conjugated secondary antibodies were purchased from BOSTER. The glutathione monoclonal antibody [D8] was purchased from Abcam. The GPX4 monoclonal antibody and xCT/SLC7A11 monoclonal antibody were purchased from Zenbio. Annexin V-FITC Apoptosis Detection Kit was purchased from Bestbio. DAPI and Crystal Violet were purchased from Solarbio Science & Technology Co. Ltd.. Cell Meter Intracellular GSH Assay Kit was purchased from AAT Bioquest. The Reduced Glutathione Assay Kit was purchased from Nanjing Jiancheng Bioengineering Institution. Dulbecco's Modied Eagle Medium (DMEM, high glucose) and DMEM (high glucose, no cystine) were purchased from Gibco (Thermo Fisher Scientific). FBS was purchased from Inner Mongolia Opcel Biotechnology Co., Ltd.. Bradford Protein Quantitation Assay Kit was purchased from Servicebio. Penicillin/streptomycin were purchased from Hyclone Laboratories, Inc.. Super ECL Detection Reagent was purchased from Yeasen Biotechnology Co., Ltd.. Immobilon®-P Membrane, PVDF, 0.45 μm was purchased from Millipore. All other reagents were of analytical grade and used as received without further purification.

Synthesis of SCACDs

Briefly, 970 mg of sulfasalazine and 3 mL of ammonia solution (25~28%) were dissolved in ultrapure water (27 mL) by sonication for 10 minutes to obtain the solution of sulfasalazine. Subsequently, 1192.5 mg of citric acid monohydrate was fully dissolved in ultrapure water (30 mL) to obtain the solution of citric acid. Then, every 6 mL of the solution of sulfasalazine and every 6 mL of the solution of citric acid were added to a Teflon-lined, stainless-steel autoclave in sequence and heated in an oven at 200 ℃ for 240 min. After the reactor was cooled to room temperature naturally, the reaction solution was filtered through a 0.22 μm microporous membrane to remove the large tracts, and a transparent brown solution was separated. The solution was first dialyzed in a dialysis bag with a molecular weight cut-off of 1 kDa against ultrapure water to remove residual small molecular species and the ammonia, and subsequently was dialyzed against diluted ammonia solution (pH ≈ 9) to fully remove residual small molecular species. Finally, the solution was dialyzed against ultrapure water again to remove the residual ammonia, and purified SCACDs were obtained. A fixed volume of the solution was taken out and freeze-dried to determine the concentration of the SCACDs.

Synthesis of PEGylated SCACDs

The SCACDs was added to the solution of DSPE-mPEG solution (1 mg mL^{-1}) with a concentration ratio of 1:4 and then sonicated for 30 min. Then, excess DSPE-mPEG was removed by dialysis, and PEGylated SCACDs were

obtained. The solution of PEGylated SCACDs was further freeze-dried for further use.

Synthesis of Cy5-SCACDs

The SCACDs was added to the solution of DSPE-PEG-Cy5 with a concentration ratio of 1:4 and then sonicated for 30 min in the dark. Then, excess DSPE-PEG-Cy5 was removed by dialysis, and Cy5-SCACDs were obtained.

Characterization

TEM imaging was done on the FEI Tecnai G^2F20 high-resolution transmission electron microscope at an acceleration voltage of 200 kV. FT-IR measurements were carried out on a BRUKER Vertex 70 FT-IR spectrometer, and 32 scans were taken with a spectral resolution of 2 cm^{-1}. The ζ potential measurements were performed on Malvern Nano ZS-90 at 25℃. XPS measurements were performed on a Thermo Fisher Scientific ESCALAB 250Xi XPS system. Confocal imaging was carried out on a Nikon A1R confocal microscope. Powder X-ray diffraction (XRD) measurement was conducted by a BRUKER D8 ADVANCE X-ray diffractometer equipped with CuKα radiation (λ=0.15406 nm). UV-vis-NIR absorbance measurements were carried out on an Agilent Cary 300 UV-Vis spectrophotometer. Fluorescence spectra were recorded on a JASCO FP-6500 spectrofluorometer. ESR analysis was conducted by BRUKER A300 electron spin resonance spectrometer by using DMPO or TEMP as trapping agents. MALDI-TOF MS analysis was recorded on a BRUKER AutoflexIII smartbeam mass spectrometer. TGA was recorded on a Perkin-Elmer Pyris Diamond TG/DTA with a heating rate of 10 ℃/minute in the temperature range of 40 ℃~905 ℃ in N_2 atmosphere. Raman spectrum was recorded on a Jobin Yvon T64000 Raman spectrometer with an excitation of 532 nm. UV-Vis diffuse reflectance spectra were carried out on a Shimadzu UV 3600 spectrophotometer.

Solid-state NMR measurements

The ^{13}C {^1H} CP MAS spectra were recorded on a Bruker AVANCE NEO 400 WB spectrometer (Bruker BioSpin AG, Fällanden, Switzerland) equipped with a 4 mm standard bore CPMAS probehead whose X channel was tuned to 100.62 MHz for ^{13}C and the other channel was tuned to 400.18 MHz for broad band ^1H decoupling, using a magnetic field of 9.39T at 297 K. The dried and finely powdered samples were packed in the ZrO_2 rotor closed with Kel-F cap which were spun at 8 kHz rate. The experiments were conducted at a contact time of 2 ms. A total of 3000 scans were recorded with 3 s recycle delay for each sample. All ^{13}C CP MAS chemical shifts are referenced to the resonances of adamantane ($C_{10}H_{16}$) standard (d_{CH2}=38.4).

Electron spin resonance spectroscopy

Electron spin resonance (ESR) spectroscopy was adopted to explore the generation of $^1O_2$ than $\cdot O_2^-$ by using TEMP and DMPO as the trapping agents, respectively. SCACDs with various concentrations were mixed with trapping

agents and exposed to US irradiation (1 MHz, 0.5 W cm^{-2}) for 0 min, 1 min, 2 min, and 5 min. The characteristic peak signals were detected by an ESR spectrometer. In these experiments, the intensities of the ESR signal were measured as the peak-to-peak height of the second line of ESR spectrum. ESR settings: microwave power: 19.23 mW, microwave frequency: 9.853616 GHz, center field: 3510.00 G, modulation frequency: 100.00 kHz; modulation amplitude: 1.00 G. The concentration of the trapping agents was 33 mM.

Cell culture

B16F10 cells were obtained from the American Type Culture Collection (ATCC) and cultured at 37 °C under 5% CO_2 in an incubator (Thermo Fisher). Media was Dulbecco's Modified Eagle Medium (DMEM, high glucose) containing FBS (10%), and penicillin/streptomycin (1%, W/V).

Cellular experiments

B16F10 cells were incubated with SCACDs for 24 h, followed by US irradiation (1 MHz, 1 W cm^{-2}) for 1 min.

Cell viability study

The cell viabilities were determined by a standard MTT assay. Briefly, B16F10 cells (5×10^3 cells per well) were seeded in 96-well plates and incubated overnight. After incubating with SCACDs for 24 h, US irradiation (1 MHz, 1 W cm^{-2}, 1 min) was conducted, and incubated for another 24 h. Then, MTT was added to the culture medium and incubated for 4 h at 37 °C in 5 % CO_2. Afterwards, 200 μL of DMSO was added to dissolve the formazan crystals, and an microplate reader (BMG LABTECH CLARIOstar®Plus) was used to measure the absorbance at 570 nm. For the comparison of the anticancer efficacy of SCACDs, P25 TiO_2, and sulfasalazine, B16F10 cells (5×10^3 cells per well) were seeded in 96-well plates and incubated overnight. After incubating with SCACDs and P25 TiO_2 for 24 h, US irradiation (1 MHz, 1 W cm^{-2}, 1 min) was conducted and incubated for another 24 h. Then, MTT was added to the culture medium and incubated for 4 h at 37 °C in 5 % CO_2. Afterwards, 200 μL of DMSO was added to dissolve the formazan crystals, and an microplate reader (BMG LABTECH CLARIOstar®Plus) was used to measure the absorbance at 570 nm. Notably, the pharmacophore content of sulfasalazine in SCACDs was calculated to be ~10.6% based on the S content in sulfasalazine as the reference. Thus, the concentration of sulfasalazine used in the experiments was 10.6% of the concentration of SCACDs used in the experiments.

To investigate the cytotoxicity of SCACDs towards normal cells, HaCaT cells (1×10^4 cells per well) were seeded in 96-well plates and incubated overnight. After incubating with SCACDs for 24 h, MTT was added to the culture medium and incubated for 4 h at 37 °C in 5 % CO_2. Afterwards, 200 μL of DMSO was added to dissolve the formazan crystals, and an microplate reader (BMG LABTECH CLARIOstar®Plus) was used to measure the absorbance at 570 nm. Moreover, HaCaT cells (5×10^3 cells per well) were seeded in 96-well plates and incubated

overnight. After incubating with SCACDs for 72 h, MTT was added to the culture medium and incubated for 4 h at 37 °C in 5 % CO_2. Afterwards, 200 μL of DMSO was added to dissolve the formazan crystals, and an microplate reader (BMG LABTECH CLARIOstar®Plus) was used to measure the absorbance at 570 nm.

Cellular uptake

B16F10 cells with a density of 5×10^4 cells per well were seeded in a 6-well plate and incubated overnight. After 24 h attachment, cells were treated with Cy5-SCACDs (25 μg/mL) for different periods and cellular fluorescence imaging was performed on a Nikon A1R confocal microscope.

Colony formation assay

B16F10 cells (5×10^5 cells per well) were seeded in 6-well plates and incubated overnight. After incubating with SCACDs (25 μg/mL) for 24 h, US irradiation (1 MHz, 1 W cm^{-2}, 1 min) was conducted. Single-cell suspension from various groups (5×10^2 cells per well) was seeded in 6-well plates and incubated for 14 days, and the culture medium was changed once every three days. After being washed with PBS twice, cells were fixed with 4% paraformaldehyde for 20 minutes at room temperature. Then, the cells were stained with crystal violet. Images were collected by an EPSON scanner.

Cystine uptake analysis

B16F10 cells (1×10^4 cells per well) were seeded in 96-well plates and incubated overnight. After incubating with SCACDs (25 μg/mL) for 24 h, the cells were further incubated in cystine-free DMEM for 1 h, and the cystine uptake of the B16F10 cells was determined by a Cystine Uptake Assay Kit (DOJINDO Laboratories) according to the manufacturer's instructions.

ROS detection

Intracellular ROS level was detected by flow cytometry (BD LSRFortessa Cell Analyzer) by using DCFH-DA as the fluorescent indicator. Briefly, B16F10 cells (5×10^5 cells per well) were seeded in 6-well plates and incubated overnight. After incubating with SCACDs (25 μg/mL) for 24 h, cells were stained with DCFH-DA for 20 min at 37 ℃ in 5% CO_2, and US irradiation (1 MHz, 1 W cm^{-2}, 1 min) was conducted. Then, the cells were collected for flow cytometry analysis of fluorescence detection.

GSH detection by the Cell Meter Intracellular GSH Assay

B16F10 cells (5×10^5 cells per well) were seeded in 6-well plates and incubated overnight. After incubating with SCACDs for 24 h, intracellular GSH content was measured using the Cell Meter Intracellular GSH Assay Kit according to manufacturer's protocol using flow cytometer (BD LSRFortessa Cell Analyzer) and the Olympus fluorescence microscope.

GSH detection by the Reduced Glutathione Assay Kit

B16F10 cells (5×10^5 cells per well) were seeded in 6-well plates and incubated overnight. After incubating with SCACDs for 24 h. The concentration of intracellular GSH was detected by the Reduced Glutathione Assay Kit according to the manufacturer's instructions.

Apoptosis assay

Cell apoptosis assays were performed using the Annexin V-FITC Apoptosis Detection Kit following the manufacturer's instructions. B16F10 cells (5×10^5 cells per well) were seeded in 6-well plates and incubated overnight. After incubating with SCACDs (25 μg/mL) for 24 h, US irradiation (1 MHz, 1 W cm^{-2}, 1 min) was conducted. Afterwards, cells were stained with Annexin V-FITC and Propidium Iodide (PI) for 15 min at 37 ℃ in 5% CO_2, and subsequently collected and analyzed by flow cytometry (BD LSRFortessa Cell Analyzer).

Western blotting

Samples were first lysed in RIPA buffer supplemented with protease inhibitor cocktail at 4 °C, and the protein concentration was determined by a Bradford Protein Quantitation Assay Kit. Afterward, 25 μg of protein from each sample was resolved by SDS-PAGE (8%-10% SDS-PAGE gels), and subsequently transferred to the polyvinylidene difluoride (PVDF) membranes. Membranes were then blocked in 5 % skim milk in TBST and probed with specific primary antibodies. HRP-conjugated secondary antibodies (1:10000) and ECL Chemiluminescence Detection Kit was used for protein detection. The level of β-actin or GAPDH immunoreactivity was used as a control to monitor equal protein loading.

Immunoprecipitation analysis

Cells were lysed at 4°C in ice-cold RIPA buffer and cell lysates were cleared by brief centrifugation (13,000 g, 15 min). Concentrations of proteins in the supernatant were determined using the brandford assay. Prior to immunoprecipitation, samples containing equal amounts of proteins were pre-cleared with protein Anti-Rabbit Nanobody Magarose beads (AlpalifeBio, KTSM1344, 4°C, 30 min), and subsequently incubated with various irrelevant IgG or specific antibodies (5 μg/mL) overnight at 4°C with gentle shaking, which were further incubated with the Anti-Rabbit Nanobody Magarose beads for 1h. Finally, the Magarose beads were washed extensively with Wash buffer and proteins were eluted by boiling in 2 × sodium dodecyl sulfate sample buffer before sodium dodecyl sulfate polyacrylamide gel electrophoresis.

Hemolysis test of SCACDs

400 μL of the whole blood was collected in tubes containing EDTA-K2 from the orbital venous of mice (female Kunming mice). Then, blood samples were mixed with the proper amount of PBS (10 mM, pH = 7.4), centrifuged

for 5 min at 3000 rpm and discarded the supernatant, and repeated 3~4 times until the supernatant became colorless transparent. The precipitated erythrocytes were dispersed in 4 mL PBS (10 mM, pH = 7.4) to get erythrocyte suspensions. The SCACDs and erythrocyte suspensions were added to the PBS (10 mM, pH = 7.4) respectively to obtain a final concentration of SCACDs as 12.5 μg mL^{-1}, 25 μg mL^{-1}, 50 μg mL^{-1}, 100 μg mL^{-1}, and 200 μg mL^{-1}, and only erythrocyte suspension was added in 10 mM PBS (pH = 7.4) to get the negative control, and the positive control was erythrocyte suspension diluted with ultrapure water. The tubes were incubated for 8 h at 4 ℃, and the hemolysis phenomenon was observed and recorded. Meanwhile, the above mixtures were centrifuged, and the absorbance of the supernatants at 540 nm was determined by UV-Vis spectroscopy. Calculation of the hemolysis rate (HR%): HR% = $(A_{SCACDs}-A_{NC})$ * 100%/$(A_{PC}-A_{NC})$, where A_{SCACDs}, A_{PC}, and A_{NC} were the absorbance of the sample, the positive control, and the negative control, respectively.

Animals

Male C57BL/6 mice (ca. 25 g, 6-8 weeks), male C57BL/6 mice (ca. 20 g, 4-6 weeks), and female Kunming mice (ca. 30 g, 6-8 weeks) were purchased from the Laboratory Animal Center of Jilin University (Changchun, China). All animal procedures were performed in accordance with the Guidelines for Care and Use of Laboratory Animals of Changchun Institute of Applied Chemistry Chinese Academy of Sciences and approved by Institutional Animal Care and Use Committee of Changchun Institute of Applied Chemistry Chinese Academy of Sciences (Permit Number: 20220102).

***In vivo* biosafety of SCACDs**

Healthy male C57BL/6 mice (ca. 20 g, 4-6 weeks) were randomly divided into two groups. The mice without any treatments were defined as the control group, and the mice with intravenous injection of SCACDs (24 mg kg^{-1}, once every three days, a total of 4 times) were defined as the test group. The body weight of mice was measured every five day to evaluate the *in vivo* biosafety of SCACDs continuously. 15 days later, the blood of mice in above two groups was collected and the samples were used to perform blood biochemistry and hematology analysis. Moreover, the major organs including heart, liver, spleen, lung, and kidney were harvested, fixed with 4% paraformaldehyde, processed into paraffin, sectioned, and stained with hematoxylin and eosin (H&E).

B16F10 tumor-bearing mouse model

The tumor-bearing mouse model was established first. B16F10 cells (5×10^5 cells) were suspended in 100 μL of cell culture medium and subcutaneously injected on the back of mice. Then, tumor volume was calculated as (tumor length) × $(\text{tumor width})^2$ × 0.5.

Biodistribution analysis.

For biodistribution analysis, B16F10 tumor-bearing mice were intravenously injected with Cy5-SCACDs. Afterwards, mice were sacrificed and major organs and tumors were collected and imaged at different expected time points. Images were analyzed *via* ImageJ Software.

***In vivo* therapeutic efficacy**

Tumor-bearing mice were randomly divided into five groups and defined as control, US, sulfasalazine, SCACDs, and SCACDs + US, respectively. Then, mice were intravenously injected with sulfasalazine (6 mg kg^{-1}) or SCACDs (6 mg kg^{-1}) and repeated every three days until repeated for 4 times. At 12 h, 36 h, and 60 h post-injection of SCACDs, the mice in the US group and SCACDs + US group were irradiated with US (1 MHz, 2 W cm^{-2}, 3 min). Tumor volumes were measured by using an electronic digital caliper after various treatments. The tumor sizes and body weights were recorded for 14 days. Mice were euthanized when the tumor length reached 15 mm.

Histological analysis.

Tumor-bearing mice were randomly divided into five groups and defined as control, US, sulfasalazine, SCACDs, and SCACDs + US, respectively. Then, mice were intravenously injected with sulfasalazine (6 mg kg^{-1}) or SCACDs (6 mg kg^{-1}). At 12 h, 36 h, and 60 h post-injection of SCACDs, the mice in the US group and SCACDs + US group were irradiated with US (1 MHz, 2 W cm^{-2}, 3 min). At 72 h post-injection of SCACDs, mice in above experimental groups were sacrificed and tumors were collected for histological analysis. Harvested tumors were fixed with paraformaldehyde (4%), dehydrated, embedded in paraffin sectioned, and stained with H&E or TUNEL. Slides were observed on an Olympus optical system or a confocal microscope (Nikon A1R). Moreover, the tumors of the mice in the control group, the SCACDs group, and the sulfasalazine group were collected for immunofluorescence staining analysis.

Immunofluorescence staining

Sections were blocked in 5% goat serum for 2 h and then stained overnight at 4 °C with primary antibodies including glutathione monoclonal antibody and GPX4 polyclonal antibody. Afterwards, DyLight 488-conjugated secondary antibody or DyLight 550-conjugated secondary antibody were incubated with the above sections for 2 h. Finally, samples were imaged by a confocal microscope (Nikon A1R).

Statistical analysis

All data were expressed as mean ± standard deviation (SD) and performed in at least 3 specimens. Student's *t*-test was used for a comparison between the two groups by using GraphPad Prism 9.0 software. A P-value < 0.05 was considered statistically significant. For Figure 5b, 5c, 5g, Figure 6a-c, and Figure S16, the group of the control or NC is regarded as the control group for statistical analysis.

II. Figures

Fig. S1. Typical digital photograph of sulfasalazine (left), citric acid (middle), and SCACDs (right) powders.

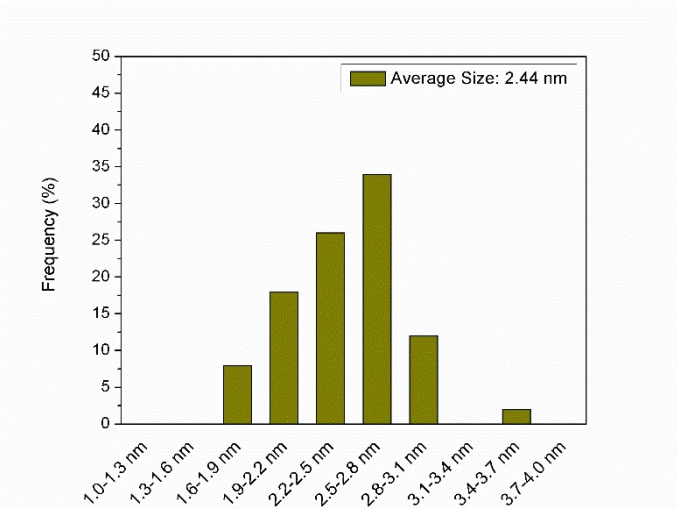

Fig. S2. Size distributions of SCACDs. The average size is 2.44 nm.

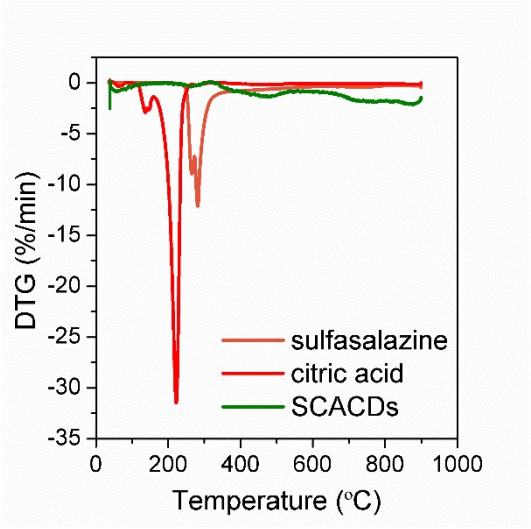

Fig. S3. The DTG profiles sulfasalazine, citric acid, and SCACDs.

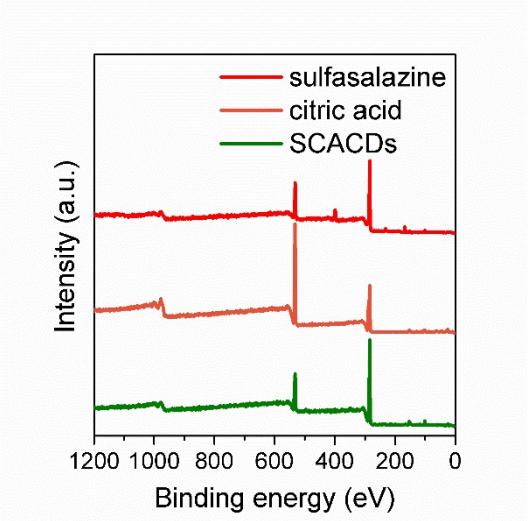

Fig. S4. The XPS survey spectra of sulfasalazine, citric acid, and SCACDs.

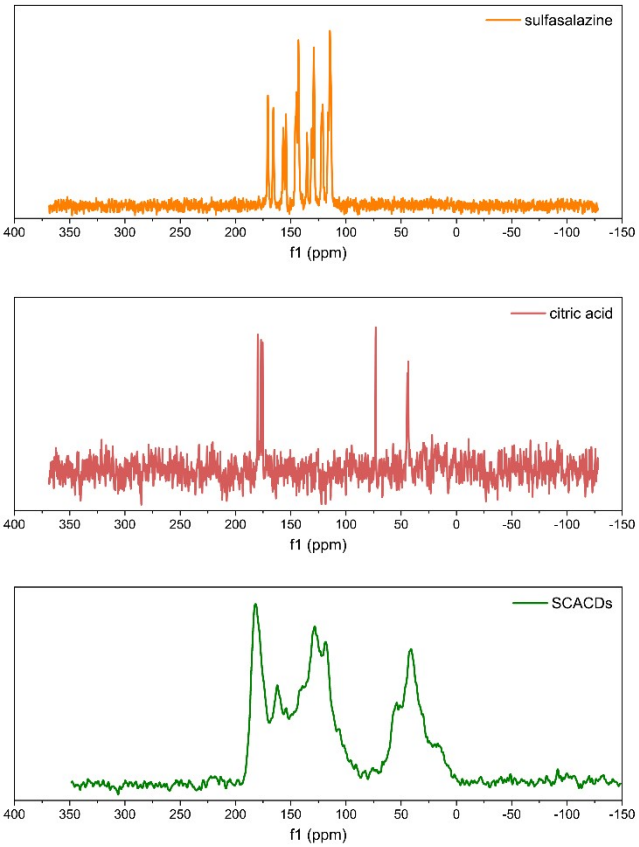

Fig. S5. The CP/MAS ^{13}C NMR spectra of sulfasalazine, citric acid, and SCACDs.

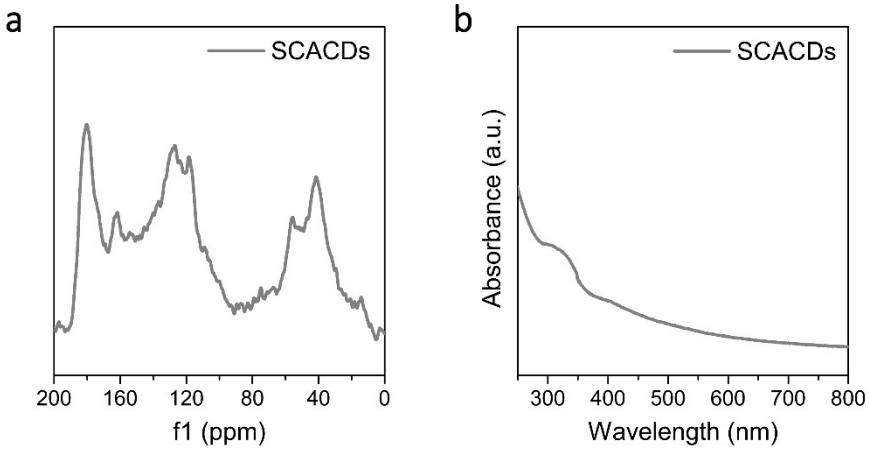

Fig. S6. The stability of SCACDs. The CP/MAS ^{13}C NMR spectrum (a) as well as the UV-Vis spectrum of SCACDs are recorded after storing in water for 6 months.

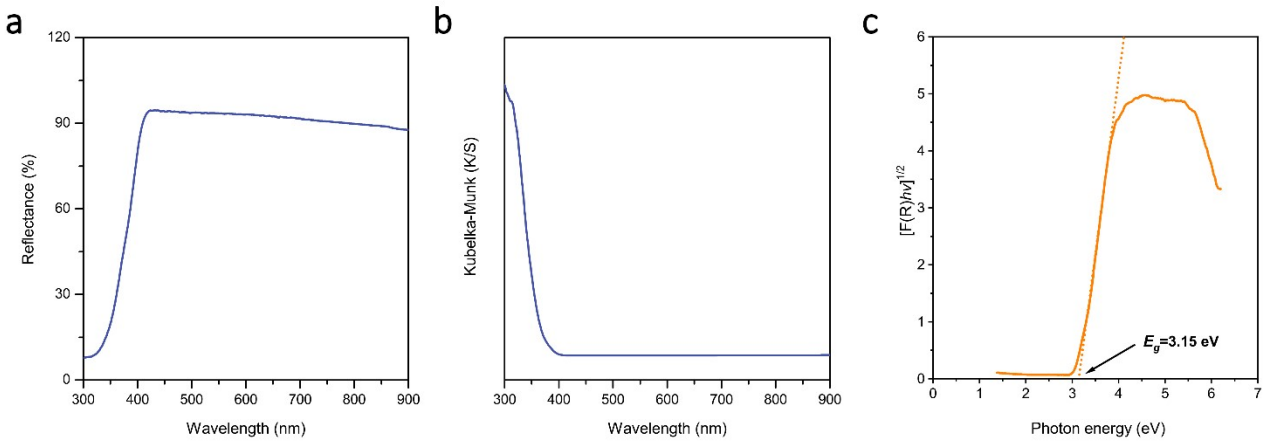

Fig. S7. (a) UV-Vis-DRS spectrum of P25 TiO_2. (b) The absorption spectrum of P25 TiO_2 transformed from the UV-Vis-DRS spectrum by using the Kubelka-Munk function. (c) Tauc plots for P25 TiO_2.

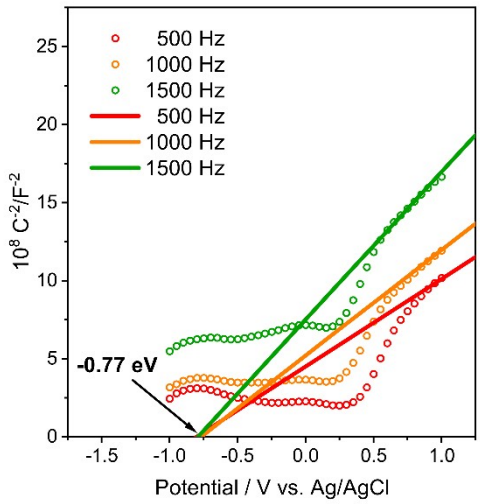

Fig. S8. Mott-Schottky plots for P25 TiO_2 in 0.5 M Na_2SO_4 aqueous solution at frequencies of 500 Hz, 1000 Hz, and 1500 Hz. The Efb determined from the intersection is approximately -0.77 V versus Ag/AgCl (-0.573 V versus NHE). Thus, the CB of P25 TiO_2 could be estimated to be -0.673 V versus NHE. Moreover, the Tauc plots results as shown in **Fig. S7c** indicated that the bandgap energy of TiO_2 was approximately 3.15 eV, thus the valence band (VB) of TiO_2 could be calculated to be 2.477 V versus NHE.

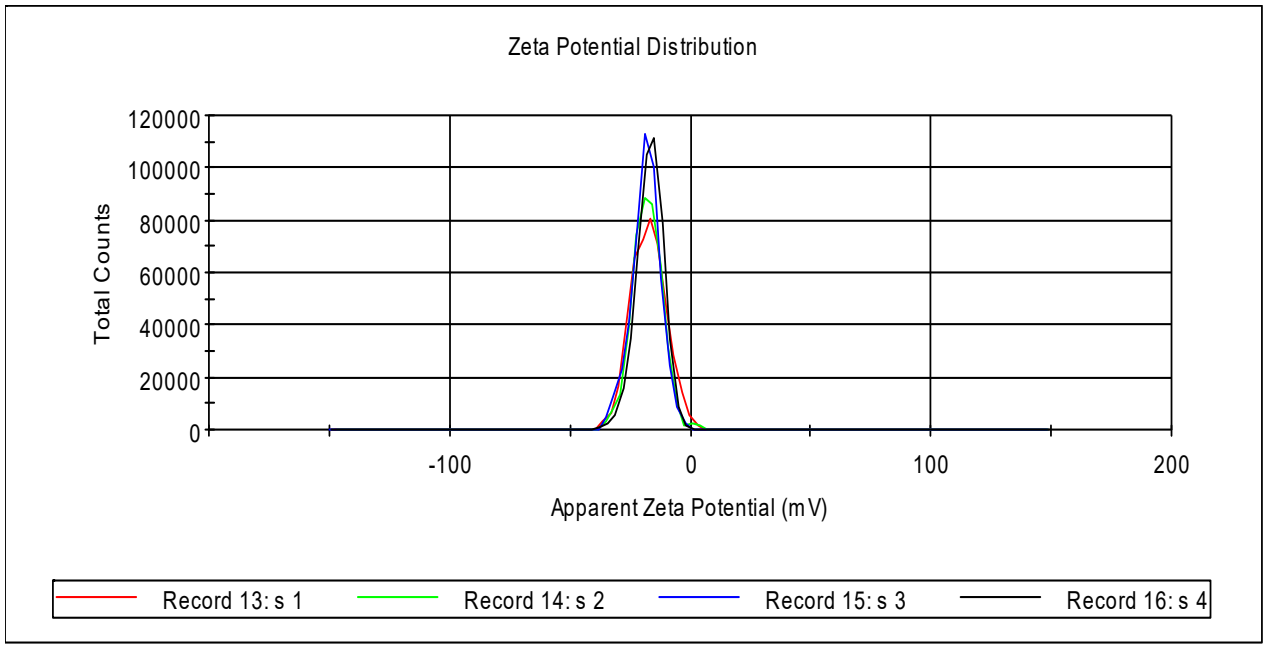

Fig. S9. The ζ potential distributions of SCACDs without PEGylation.

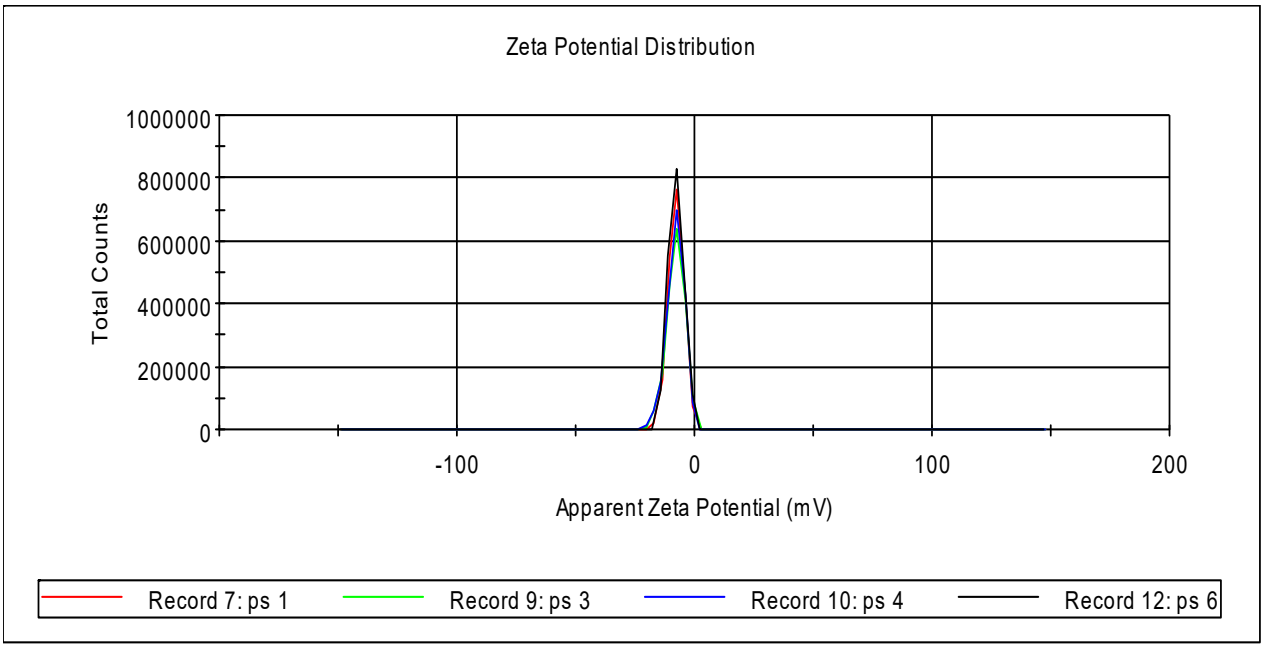

Fig. S10. The ζ potential distributions of SCACDs with PEGylation.

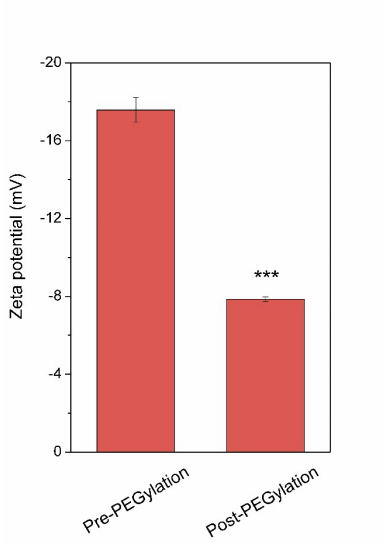

Fig. S11. The ζ potential values of SCACDs with or without PEGylation. Error bars represent standard deviation from the mean (n = 4). Asterisks indicate statistically significant differences (*$P < 0.05$, **$P < 0.01$, and ***$P < 0.001$).

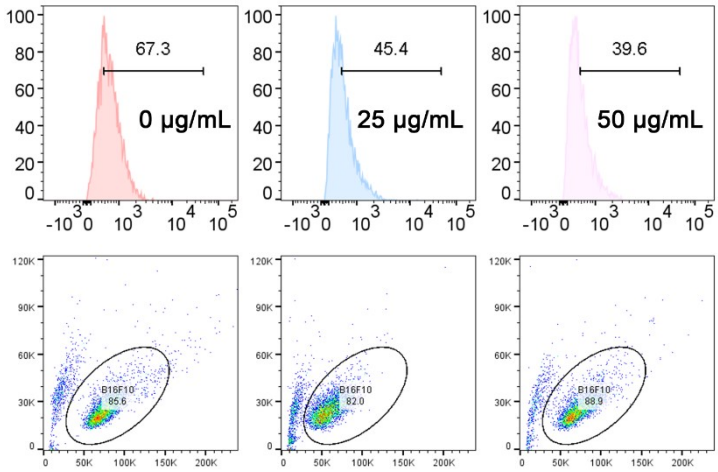

Fig. S12. Flow cytometry analysis of the GSH levels in B16F10 cells after incubating with different concentrations of SCACDs. The decreased fluorescence intensity in the flow cytometry analysis indicates the decreased intracellular GSH level.

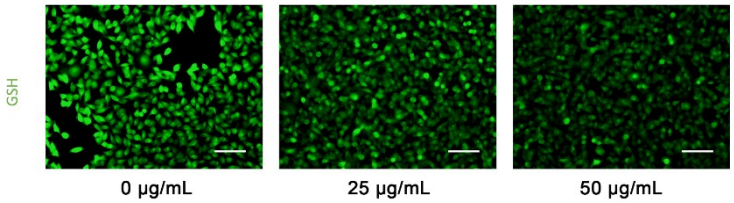

Fig. S13. The use of the Cell Meter Intracellular GSH Assay Kit to detect the GSH levels in B16F10 cells after incubating with different concentrations of SCACDs. Scale bars are equal to 100 μm. The decreased fluorescence intensity in the images indicates the decreased intracellular GSH level.

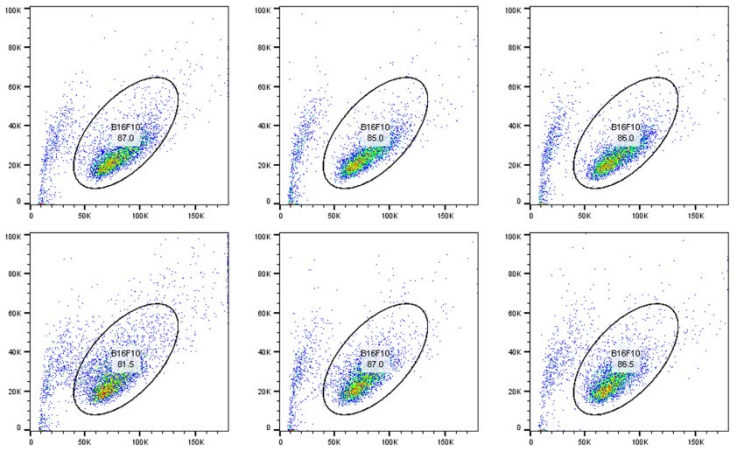

Fig. S14. Related to Figure 5d. Flow cytometry analysis of US-triggered ROS generation in B16F10 cells after various treatments. US parameters: 1.0 MHz, 1 W cm^{-2}, 1 min.

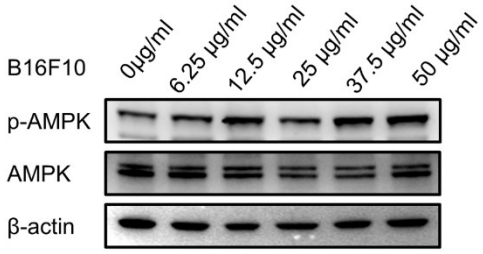

Fig. S15. Concentration-dependent of Western blot analysis of B16F10 cells after treating with SCACDs.

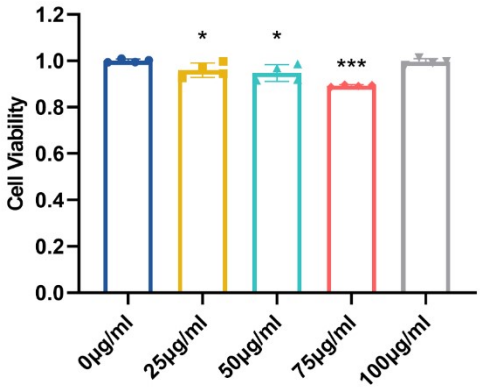

Fig. S16. Viability of HaCaT cells after incubating with various concentrations of SCACDs for 3 days. Error bars represent standard deviation from the mean (n = 4). Asterisks indicate statistically significant differences (*P < 0.05, **P < 0.01, and ***P < 0.001).

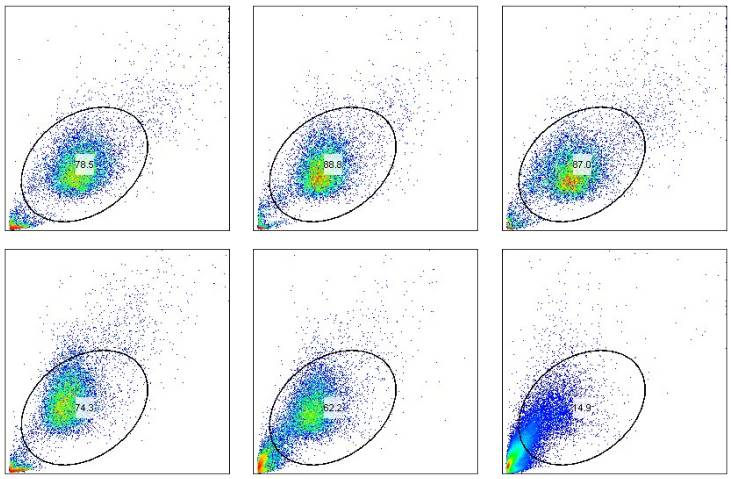

Fig. S17. Related to Figure 6e. Apoptosis/necrosis analysis of B16F10 cells after various treatments based on flow cytometry.

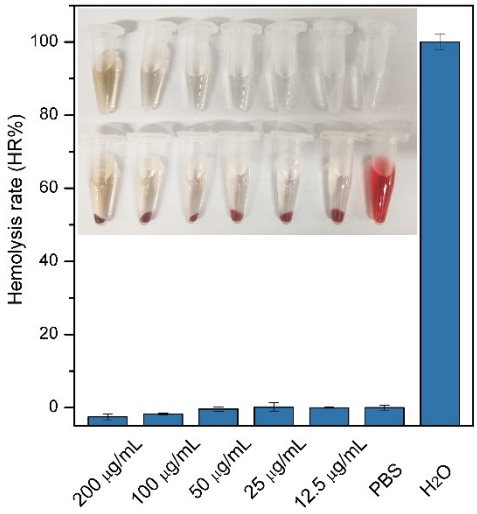

Fig. S18. Results of hemolytic assay. Concentration-dependent hemolysis of SCACDs. Inset: typical digital photographs of concentration-dependent hemolysis of SCACDs. From top to bottom: SCACDs with various concentrations; concentration-dependent hemolysis of SCACDs. From left to right: hemolysis of SCACDs under concentrations of 200 μg SCACDs mL^{-1}, 100 μg SCACDs mL^{-1}, 50 μg SCACDs mL^{-1}, 25 μg SCACDs mL^{-1}, 12.5 SCACDs mL^{-1}, PBS (the negative control) and ultrapure H_2O (the positive control). Error bars represent standard deviation from the mean (n = 3).

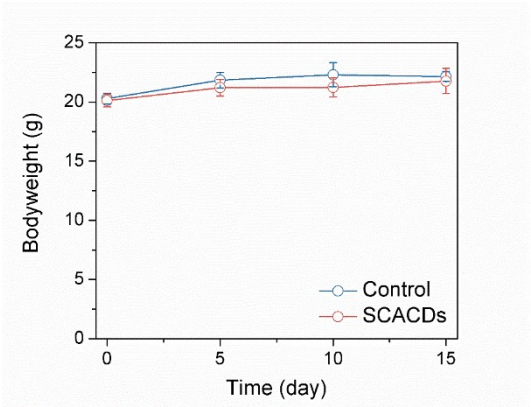

Fig. S19. Bodyweight changes of the mice after different treatments. For the SCACDs group, the mice were intravenously injected with SCACDs (24 mg kg^{-1}, once every three days, a total of 4 times). Error bars represent standard deviation from the mean (the control group, n = 5; the SCACDs group, n = 6).

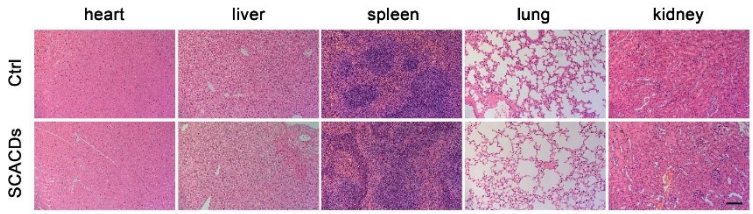

Fig. S20. H&E-stained images of the slices of the major organs collected from different experimental groups. For the SCACDs group, the mice were intravenously injected with SCACDs (24 mg kg^{-1}, once every three days, a total of 4 times). Scale bar is equal to 100 μm.

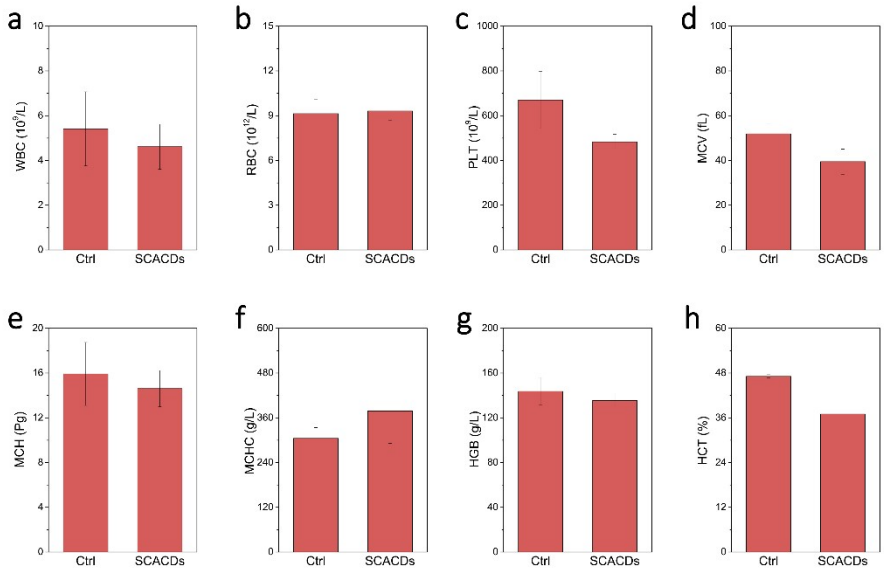

Fig. S21. Results of hematological analysis. Hematological analysis of the healthy mice after intravenously injected with SCACDs (24 mg kg^{-1}, once every three days, a total of 4 times). The blood samples were collected at 15-day post-injection. WBC, white blood cells; RBC, red blood cells; PLT, platelets; MCV, mean corpuscular volume; MCH, mean corpuscular hemoglobin; MCHC, mean corpuscular hemoglobin concentration; HGB, hemoglobin; HCT, hematocrit. Error bars represent the standard deviation from the mean (n = 3).

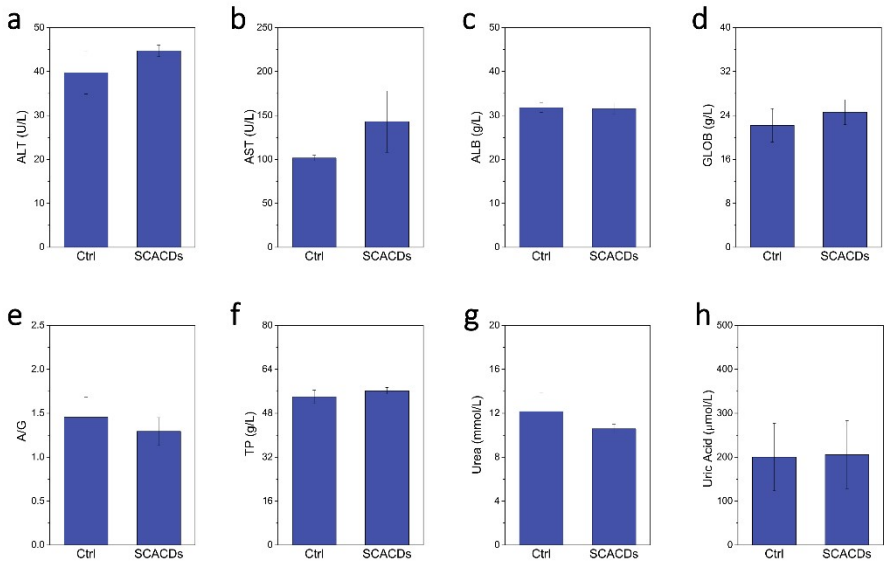

Fig. S22. Results of blood biochemical analysis. Blood biochemical analysis of the healthy mice after intravenously injected with SCACDs (24 mg kg^{-1}, once every three days, a total of 4 times). The blood samples were collected at 15-day post-injection. ALT, alanine aminotransferase; AST, aspartate aminotransferase; ALB, albumin; GLOB, globulin; A/G, albumin/globulin; TP, total protein; Urea, serum urea; Uric Acid: serum uric acid. Error bars represent the standard deviation from the mean (n = 3).

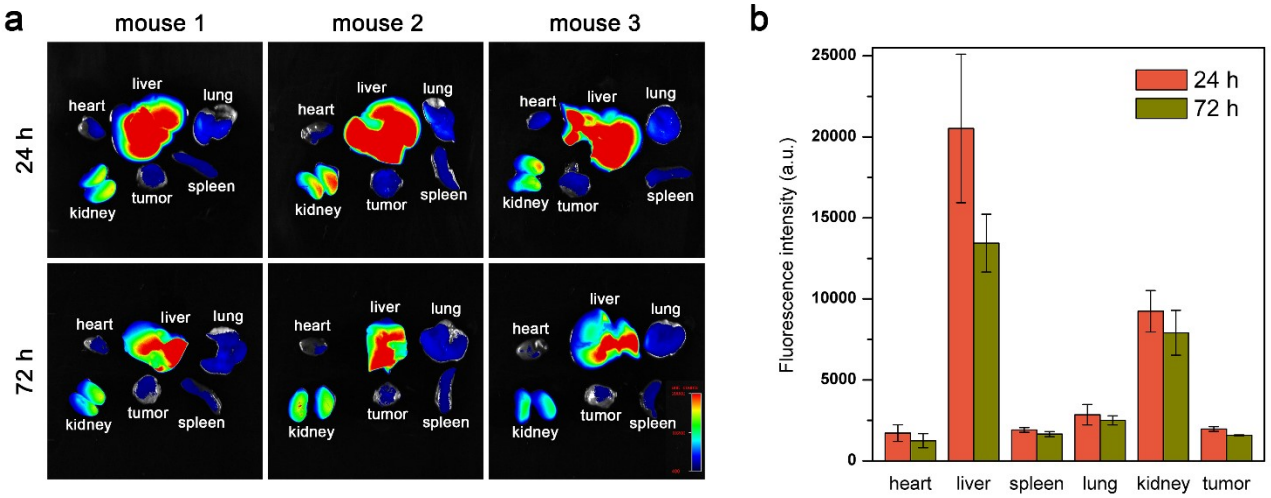

Fig. S23. Biodistributions of SCACDs. (a) Time-dependent *ex vivo* fluorescence imaging of B16F10 tumor-bearing mice after intravenous injection of Cy5-SCACDs. (b) Biodistributions of Cy5-SCACDs. Error bars represent the standard deviation from the mean (n = 3).

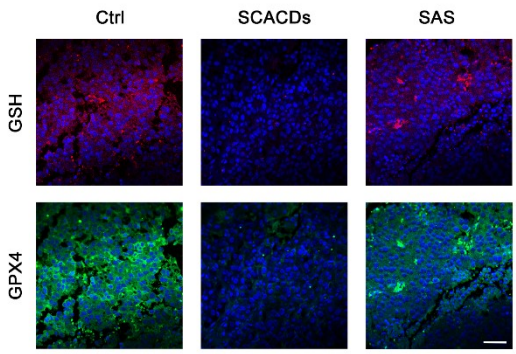

Fig. S24. GSH- and GPX4-stained immunofluorescence images of tumor slices collected from various groups. Scale bar is equal to 50 μm.

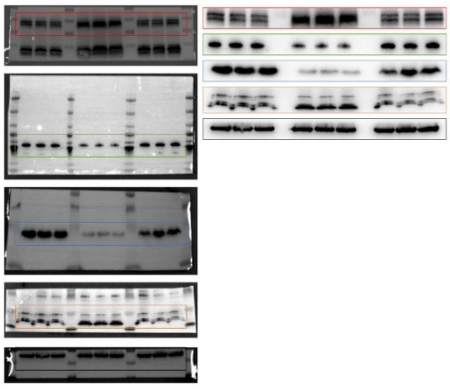

Fig. S25. Related to **Fig. 5f**. The immunoblot bands in the colored box of the uncropped western blot images are the raw data of the processed western blot data marked by the box of the same color.

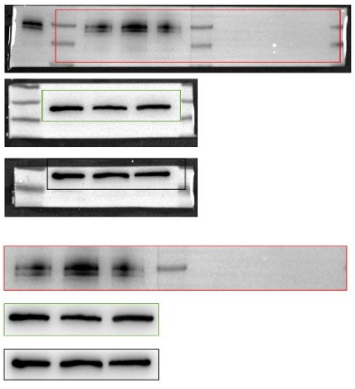

Fig. S26. Related to **Fig. 5h**. The immunoblot bands in the colored box of the uncropped western blot images are the raw data of the processed western blot data marked by the box of the same color.

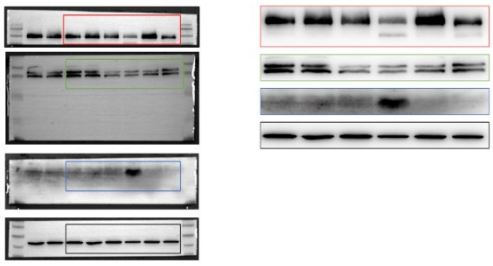

Fig. S27. Related to **Fig. 6f**. The immunoblot bands in the colored box of the uncropped western blot images are the raw data of the processed western blot data marked by the box of the same color.

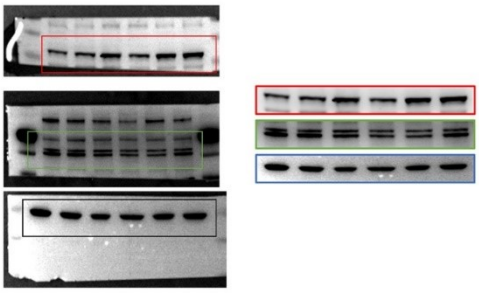

Fig. S28. Related to **Fig. S15**. The immunoblot bands in the colored box of the uncropped western blot images are the raw data of the processed western blot data marked by the box of the same color.

Table S1. The chemical shifts of different C atom on the sulfasalazine molecules with three different structures calculated by B97-2 or revTPSS functional, and their average values in terms of Boltzmann thermal distribution of these three structures. Exp represents the chemical shifts by experimental NMR characterization.

No.	B972-1	Rev-1	B972-2	Rev-2	B972-3	Rev-3	Average	Exp
C1	120.838	117.527	122.420	119.156	122.561	119.204	119.084	114.53
C2	142.536	138.105	144.513	139.988	145.031	140.026	139.898	143.04
C3	112.271	109.992	114.287	111.997	114.733	112.023	111.894	114.53
C4	156.574	154.346	157.938	155.052	158.093	154.925	154.956	156.78
C5	152.988	148.920	154.565	150.382	154.803	150.381	150.298	156.78
C6	143.564	140.497	150.278	147.463	150.600	147.637	147.143	144.66
C7	134.036	130.541	133.056	129.455	134.035	129.879	129.704	130.99
C8	117.302	114.627	117.763	115.236	138.812	135.402	124.115	122.03

C9	157.133	153.538	158.668	154.963	158.893	155.047	154.919	154.38
C10	137.122	133.913	138.310	135.167	117.831	114.993	126.179	122.03
C11	133.409	129.648	138.098	133.872	137.124	133.201	133.335	130.99
C12	146.569	144.028	149.371	146.658	149.182	146.449	146.416	145.56
C13	119.779	116.185	144.239	139.845	122.009	117.932	128.811	122.03
C14	111.404	109.482	112.693	110.650	112.960	110.879	110.685	114.53
C15	170.703	167.567	174.603	171.063	173.922	170.343	170.546	165.78
C16	121.593	119.021	123.706	121.447	123.126	120.425	120.857	121.08
C17	147.175	142.774	129.172	125.337	149.741	144.765	134.918	129.06
C18	174.288	171.410	178.285	174.987	179.270	175.885	175.180	170.59

References

1. Kühne, T.D. *et al.* CP2K: An electronic structure and molecular dynamics software package - Quickstep: Efficient and accurate electronic structure calculations. *J. Chem. Phys.* **152**, 194103 (2020).
2. Bonomi, M. *et al.* Promoting transparency and reproducibility in enhanced molecular simulations. *Nat. Methods* **16**, 670-673 (2019).
3. Perdew, J.P., Burke, K. & Ernzerhof, M. Generalized Gradient Approximation Made Simple. *Phys. Rev. Lett.* **77**, 3865-3868 (1996).
4. Grimme, S., Antony, J., Ehrlich, S. & Krieg, H. A consistent and accurate ab initio parametrization of density functional dispersion correction (DFT-D) for the 94 elements H-Pu. *J. Chem. Phys.* **132**, 154104 (2010).
5. Grimme, S., Bannwarth, C. & Shushkov, P. A Robust and Accurate Tight-Binding Quantum Chemical Method for Structures, Vibrational Frequencies, and Noncovalent Interactions of Large Molecular Systems Parametrized for All spd-Block Elements (Z = 1–86). *J. Chem. Theory Comput.* **13**, 1989-2009 (2017).
6. Laio, A. & Parrinello, M. Escaping free-energy minima. *Proc. Natl. Acad. Sci. U. S. A.* **99**, 12562-12566 (2002).
7. Pietrucci, F. & Andreoni, W. Graph Theory Meets Ab Initio Molecular Dynamics: Atomic Structures and Transformations at the Nanoscale. *Phys. Rev. Lett.* **107**, 085504 (2011).
8. Frisch, M.J. *et al. Gaussian 16 Rev. C.01* (2016).
9. Wolinski, K., Hinton, J.F. & Pulay, P. Efficient implementation of the gauge-independent atomic orbital method for NMR chemical shift calculations. *J. Am. Chem. Soc.* **112**, 8251-8260 (1990).
10. Chesnut, D.B. & Moore, K.D. Locally dense basis sets for chemical shift calculations. *J. Comput. Chem.* **10**, 648-659 (1989).
11. Marenich, A.V., Cramer, C.J. & Truhlar, D.G. Universal Solvation Model Based on Solute Electron Density and on a Continuum Model of the Solvent Defined by the Bulk Dielectric Constant and Atomic Surface Tensions. *J. Phys. Chem. B* **113**, 6378-6396 (2009).
12. Humphrey, W., Dalke, A. & Schulten, K. VMD: Visual molecular dynamics. *J. Mol. Graph.* **14**, 33-38 (1996).
13. Lu, T. & Chen, F. Multiwfn: A multifunctional wavefunction analyzer. *J. Comput. Chem.* **33**, 580-592 (2012).